

# Simulating cortical network activity states constrained by intracellular recordings

Fabián P. Alvarez <sup>a,b</sup> and Alain Destexhe <sup>a</sup>

<sup>a</sup>*Unité de Neurosciences Intégratives et Computationnelles, CNRS, Bat. 33,  
Avenue de la Terrasse 1, 91198 Gif-sur-Yvette, France*

<sup>b</sup>*Sec. Neurociencias, Facultad de Ciencias, Montevideo, Uruguay*

---

## Abstract

We present a method for studying states of network activity while incorporating constraints provided by intracellular measurements. Taking into account measurements of the average membrane potential, input resistance changes and membrane potential fluctuations, narrows down the possible region of parameter space (connectivity, quantal conductances) where this activity can appear in networks. Searching in those specific regions greatly enhances the efficiency of the network level modeling because irrelevant parameter combinations are automatically eliminated. We illustrate this approach by modeling self-sustained stochastic states in networks of excitatory and inhibitory neurons, based on intracellular recordings *in vivo*.

*Key words:* stochastic activity; high-conductance states; up-states; network model

---

## 1 Introduction

In mammalian neocortex, pyramidal neurons (PYs) receive thousands of synaptic connections, most of which originate from the cerebral cortex itself. During activated states *in vivo*, intracellularly-recorded PYs are in a “high-conductance state” characterized by a depolarized membrane potential ( $V_m$ ), sustained fluctuations, and a low input resistance [1,2]. This high-conductance state is mainly due to synaptic activity and has drastic consequences on integrative properties at the single-cell level [1].

To investigate the consequences of high-conductance states at the network level, the first step is to reproduce self-sustained stochastic states of activity, as found in neocortex *in vivo* during activated states [1] or during persistent activity [3]. The high degree of connectivity in neocortex, with thousands of

synaptic connections for each pyramidal neuron, together with the spontaneous (irregular) firing of a small fraction of cortical neurons, are probably responsible for generating these states through recurrent interactions, as indicated by the observation of similar states of spontaneous activity in cortical slices [4]. Indeed, a number of computational models have reported states of self-sustained stochastic activity resulting from recurrent interactions between excitatory and inhibitory neurons [5–9]. However, in none of these studies the states of the neurons were consistent with the high-conductance states measured experimentally *in vivo*.

To identify network mechanisms implicated in the genesis of such self-sustained high-conductance states, the common approach is to simulate networks and perform unconstrained variations of their connectivity and connection strength in order to map the genesis of states by such networks, and finally identify the regions of parameter space which are consistent with experimental measurements. We explore here a different approach, consisting in the use of intracellular measurements in order to obtain constraints on possible architectures in which these states are possible. This procedure allows us to considerably reduce the parameter space in network simulations and ultimately obtain states of activity consistent with intracellular measurements.

## 2 Methods

Pyramidal neurons and interneurons (INs) were simulated through classical single compartment Hodgkin-Huxley type models, but with the addition of the  $K^+$ -dependent inactivating conductance  $g_M$  for PYs. Synapses were simulated by kinetic models, taking into account AMPA, NMDA and GABA<sub>A</sub> receptor types. All models were as described in ref. [2].

Different network topologies were studied, but preserving the ratio 4:1 between PYs and INs characterized for the neocortex [10]. For the results presented here, the connections were randomly chosen at the beginning of each simulation.

## 3 Results

To constrain network simulations, we used the following measurements obtained from intracellular recordings *in vivo* [1,2]. *(i)* The resting value of the neurons after suppression of network activity was about -80 mV. *(ii)* The average  $V_m$  during network activity was about -65 mV. *(iii)* The input resistance was reduced by about 5-fold by network activity. *(iv)* The standard deviation

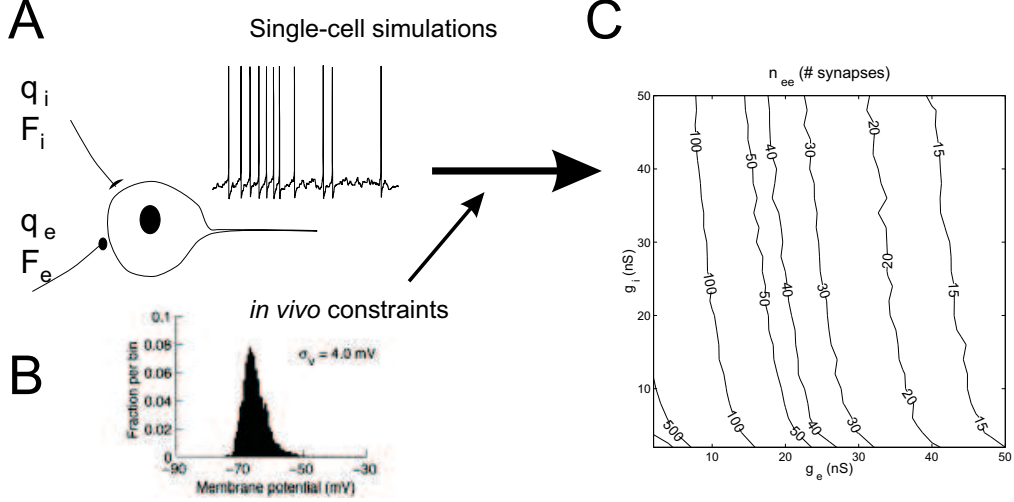


Fig. 1. **Constraining connectivities procedure.** **A.** Simulated PY receiving excitatory and inhibitory stochastic synaptic input, the output spike train is analyzed. **B.** *In vivo* measurements are used to constrain parameters of the simulated data. **C.** From simulation results, a map representing  $n_{ee}$  as a function of  $\{q_e, q_i\}$  is produced.

of the  $V_m$  was about 4 mV on average. (*v*) The average firing rate during these states was between 1 and 20 Hz.

From the passive membrane equation at steady-state, we can obtain expressions for the average  $V_m$  and the total conductance as a function of the leak ( $g_L$ ) and synaptic conductances ( $g_{exc}$  and  $g_{inh}$ ). Inserting the measurements above, one obtains that:

$$g_{exc} = 0.73 g_L, \quad g_{inh} = 3.27 g_L \quad (1)$$

In other words, these *in vivo* measurements directly show a dominance of inhibition, which conductance is about 4.5 times larger than excitatory conductances.

It is also possible to calculate the total synaptic conductance from the parameters of synaptic conductances, leading to  $g_{exc} = n_{ee} f_e Q_e$ , where  $n_{ee}$  is the number of excitatory synapses per neuron,  $f_e$  is their average release rate, and  $Q_e$  is the total conductance (integral) of a single synaptic event. Similarly, for inhibition we have  $g_{inh} = n_{ie} f_i Q_i$ . Assuming that all synapses have the same quantum ( $q_e$  for excitation and  $q_i$  for inhibition), that inputs are uncorrelated, and taking into account that the integral of an exponential synapse is  $Q_e = q_e \tau_e$ ,  $Q_i = q_i \tau_i$ , with  $\tau_e$ ,  $\tau_i$  representing their respective time constants, we obtain the set of constraints:

$$g_{exc} = n_{ee} f_e q_e \tau_e, \quad g_{inh} = n_{ie} f_i q_i \tau_i \quad (2)$$

We can now combine Eqs. (1) and (2) to derive the parameters  $n_{ee}$ ,  $n_{ie}$ ,  $q_e$ ,  $q_i$ , and  $f_i$  which allow the network to operate consistently with the experimental data obtained *in vivo*. To this end, we ran simulations of single PYs described by Hodgkin-Huxley type models (Fig. 1-A). For a given couple  $\{q_e, q_i\}$ , each neuron was subject to random synaptic activity of parameters  $F_e = n_{ee} f_e$  and  $F_i = n_{ie} f_i$ , preserving always relation (1);  $V_m$ ,  $\sigma_{V_m}$  and  $f_e$  were averaged during 100 s length simulations. These simulations were repeated for different values of  $q_e$  and  $q_i$ , both comprised between 1 and 50 nS. From all those simulations, we identified the regions producing  $V_m$  activity consistent with intracellular measurements (average  $V_m$ ,  $\sigma_{V_m}$ ), and firing rate consistent with  $f_e$  (Fig. 1-B). Given a selected couple  $\{q_e, q_i\}$ , we know the exact value of  $f_e$  for this simulation, and then, using the relation for  $g_{exc}$  in Eq.(2) we can obtain the mapping of values of  $n_{ee}$  arising from this experiment (Fig. 1-C).

These parameters of “synaptic bombardment”  $\{q_e, q_i\}$  were then tested in inhibitory INs in order to verify that the obtained firing rate is consistent with  $f_i$ . The scheme of the procedure is analogous to the one performed for the PYs. It was repeated for a large range of possible values for the number of synapses  $\{n_{ei}, n_{ii}\}$  and for the connection strength  $\{q_e, q_i\}$ , until we identified the region of parameter space where these values are all consistent with each-other.

A given set of consistent values corresponds to a given possible state at the network level, in which cellular parameters are consistent with intracellular measurements. We tested this numerically by simulating various network architectures based on the parameters determined by the single-cell analysis above. This analysis led to a continuum of possible network configurations, which range from small networks with few strong connections, up to large networks with many synapses of small quantal size. These possible network architectures were simulated numerically using the same single-neuron models as above.

In many simulations, the network activity showed a high degree of synchronization in neurons’ firing. In this case, the strong quantal conductances which would allow to reach the self-sustained stochastic states in fact originated a strong correlated input on the PYs, then invalidating the conditions assumed in our approach. However, this type of synchronized state could be avoided by introducing a longer lasting excitatory synaptic conductance, namely including NMDA receptors, which conductances were characterized by  $g_{NMDA}$ . In this case, “desynchronized” network states were more easily obtained.

A few representative examples of such network simulations are displayed in Fig. 2. The three subplots show results for networks of 2000 neurons, all of which received stochastic input until  $t = 1$  s, while only 5% of randomly chosen neurons received this random input after this time. These three examples only

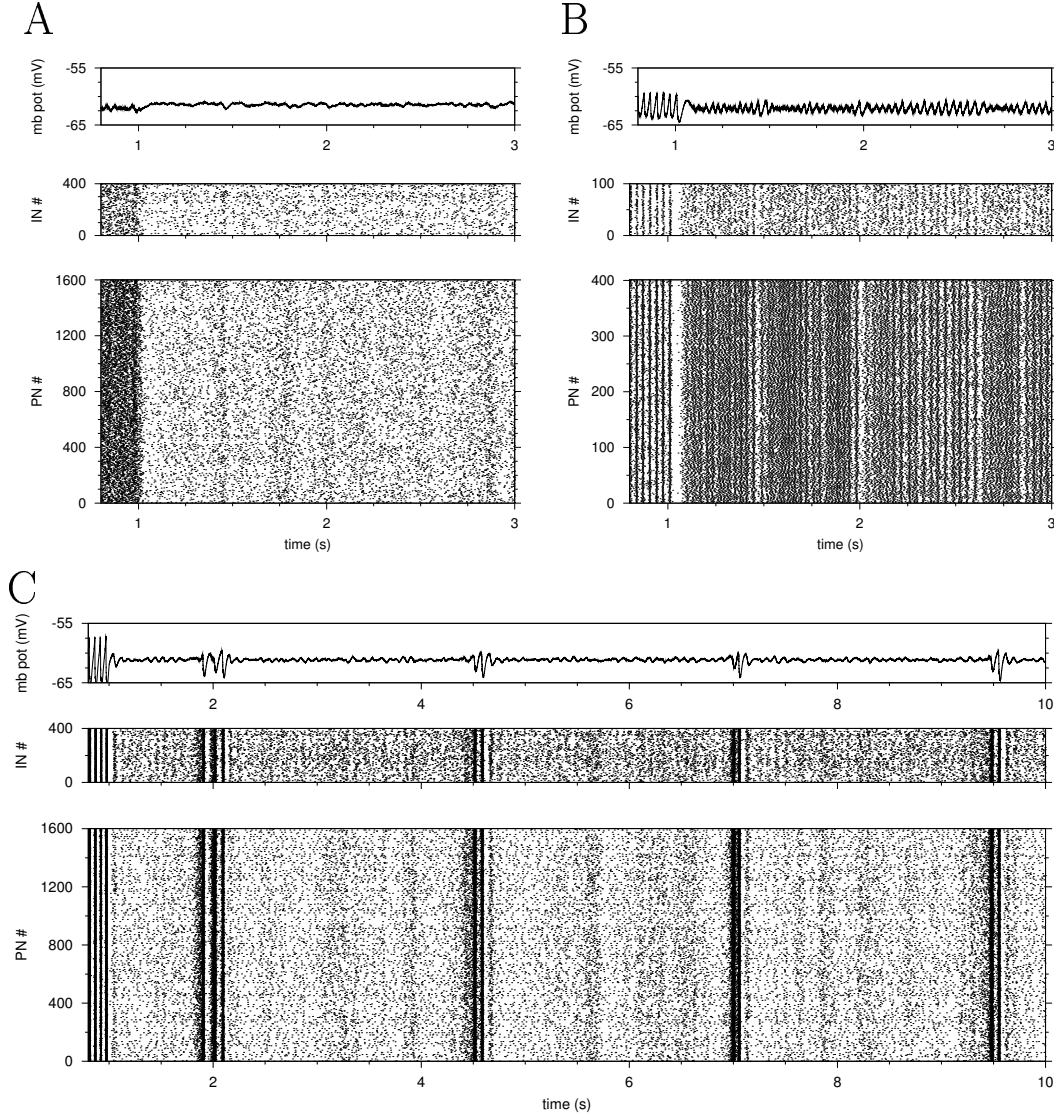


Fig. 2. **Network results.** Each subplot is made of three panels, from bottom to top: raster for PYs, raster for INs and average  $V_m$  over all the neurons. Neuron parameters as in Fig. 1. Network parameters: **A.**  $n_{ee} = 4$ ,  $n_{ii} = 4$ ,  $n_{ei} = 1$ ,  $n_{ie} = 8$ ,  $q_e = 10$  and  $q_i = 8$  nS; **B.**  $n_{ee} = 8$ ,  $n_{ii} = 4$ ,  $n_{ei} = 2$ ,  $n_{ie} = 8$ ,  $q_e = 10$ ,  $q_i = 8$  nS and  $q_{\text{NMDA}} = 4$  nS; **C.**  $n_{ee} = 16$ ,  $n_{ii} = 4$ ,  $n_{ei} = 4$ ,  $n_{ie} = 12$ ,  $q_e = 5$ ,  $q_i = 4$  nS and  $q_{\text{NMDA}} = 2$  nS.

differed from their connectivity and quantal sizes. Fig. 2-A displays the onset of a self-sustained stochastic state, where neurons fire in accordance with the *in vivo* constraints. A small increase in  $n_{ee}$  (Fig. 2-B) completely synchronized the firing of PYs for this size of network (note that only 400 PYs are shown for the sake of clarity). Finally, the third subplot (Fig. 2-C) shows the appearance of a dynamics close to slow oscillations, in which neurons alternate between quiescent and active (up-state) periods.

## 4 Conclusions

Network simulations showed that predictions for connectivity based on single neuron dynamics may work for some values of  $\{n_e, n_i\}$ , when  $n_e$  is weak compared to  $n_i$ . If the excitation is strong enough to synchronize the network, the method can not be applied because uncorrelated input was assumed in order to get the quantal values. Simulations for networks of increasing sizes up to 4000 neurons showed the augmentation of the recurrent firing as a function of size. This suggests that large networks should generate self-sustained stochastic states in which every cell is in a high-conductance state dominated by inhibitory conductances.

Research supported by HFSP and NIH.

## References

- [1] A. Destexhe, M. Rudolph, D. Paré, The high-conductance state of neocortical neurons in vivo, *Nat Rev Neurosci* 4 (2003) 739–51.
- [2] A. Destexhe, D. Paré, Impact of network activity on the integrative properties of neocortical pyramidal neurons in vivo, *J Neurophysiol* 81 (1999) 1531–47.
- [3] X. Wang, Synaptic basis of cortical persistent activity: the importance of NMDA receptors to working memory, *J Neurosci* 19 (1999) 9587–603.
- [4] M. Sanchez-Vives, D. McCormick, Cellular and network mechanisms of rhythmic recurrent activity in neocortex, *Nat Neurosci* 3 (2000) 1027–34.
- [5] N. Brunel, Persistent activity and the single-cell frequency-current curve in a cortical network model, *Network* 11 (2000) 261–80.
- [6] N. Brunel, V. Hakim, Fast global oscillations in networks of integrate-and-fire neurons with low firing rates, *Neural Comput* 11 (1999) 1621–71.
- [7] A. Compte, N. Brunel, P. Goldman-Rakic, X. Wang, Synaptic mechanisms and network dynamics underlying spatial working memory in a cortical network model, *Cereb Cortex* 10 (2000) 910–23.
- [8] A. Compte, M. Sanchez-Vives, D. McCormick, X. Wang, Cellular and network mechanisms of slow oscillatory activity (<1 Hz) and wave propagations in a cortical network model, *J Neurophysiol* 89 (2003) 2707–25.
- [9] J. Lin, K. Pawelzik, U. Ernst, T. Sejnowski, Irregular synchronous activity in stochastically-coupled networks of integrate-and-fire neurons, *Network* 9 (1998) 333–44.
- [10] V. Braitenberg, A. Schüz, *Cortex: statistics and geometry of neuronal connectivity*, Springer Verlag, Berlin, 1998 (2nd edition).